Biointerphases (2012) 7:36
DOI 10.1007/s13758-012-0036-8

ARTICLE

Enhanced Osteoblast Differentiation on Scaffolds Coated with TiO_2 Compared to SiO_2 and CaP Coatings

Anders Verket · Hanna Tiainen · Håvard J. Haugen · S. Petter Lyngstadaas · Ola Nilsen · Janne E. Reseland

Received: 25 January 2012 / Accepted: 7 May 2012 / Published online: 24 May 2012

Abstract The aim was to compare the protein release from normal human osteoblasts (NHO) cultured on scaffolds with similar morphology but different coatings. Different ceramic coatings; TiO_2, SiO_2 and calcium phosphate (CaP); $Ca_9HPO_4(PO_4)_5OH$, were applied to porous TiO_2 scaffolds prepared by polymer sponge replication. NHO were cultured on scaffolds in triplicates. The concentration of cytokines and Ca^{2+}, and alkaline phosphatase (ALP) activity in the cell media was quantified. The secretion of osteopontin, osteoprotegerin, vascular endothelial growth factor and interleukin-6 was higher from NHO on TiO_2 compared to SiO_2 and CaP. The secretion from cells on the three scaffolds was, however, either similar or lower than the control cells cultured on plastic. The Ca^{2+} concentration was higher in cell media on CaP the first week, and no difference in ALP activity was observed. TiO_2 coating induced a higher secretion of factors indicating enhanced osteoblast differentiation as compared to CaP and SiO_2.

1 Introduction

Autologous bone grafts have long been considered the 'gold standard' for reconstruction of bone due to immunological feasibility and osteoinductive properties [1]. Disadvantages of grafting with autologous bone may be limited supply of bone suitable for harvest and potential donor site morbidity [2]. These factors have led to alternative approaches of bone substitute grafting.

A scaffold for bone repair must be biocompatible. In addition, it must have osteoconductive properties, preferably with a structure mimicking trabecular bone. Further the scaffold must provide immediate physical support in order to prevent collapse of the bony defect due to potential high loads to the reconstructed site [3, 4]. It is important that the scaffolds are porous and provide a high interconnectivity in order to facilitate angiogenesis, osteoblast ingrowth and attachment [3, 5]. Various synthetic bone graft materials have been developed to fulfill these criteria in order to serve as a scaffold to promote proliferation of host osteoblasts and bone growth.

Calcium phosphates (CaP), hydroxyapatite (HA) and β-tricalcium phosphate (β-TCP) in particular, have been extensively researched and widely used for bone repair as it represents the main inorganic constituent in hard tissues and possesses osteoconductive properties [6]. Further, certain types of calcium phosphates have demonstrated osteoinductive properties [7, 8], although these mechanisms are unclear [6]. Bioactive glasses represent another type of biomaterial with osteoinductive properties [9], and a porous Bioglass® scaffold for bone repair has recently been developed [10]. However, common for calcium phosphates and bioactive glasses is low compressive strength in scaffolds designed with the porosity and interconnectivity required for bone ingrowth [10–13]. These mechanical limitations may impede scaffold use for bone repair in load bearing sites.

Titanium dioxide (TiO_2) is a biocompatible material reported to have bioactive properties [14, 15]. In addition, the TiO_2 scaffolds have demonstrated compressive strength

A. Verket (✉) · H. Tiainen · H. J. Haugen · S. P. Lyngstadaas · J. E. Reseland
Department of Biomaterials, Institute of Clinical Dentistry, University of Oslo, P.O. Box 1109, Blindern, 0317 Oslo, Norway
e-mail: anderver@odont.uio.no
URL: http://www.biomaterials.no

O. Nilsen
Department of Chemistry, Centre for Materials Science and Nanotechnology, University of Oslo, P.O. Box 1033, Blindern, 0315 Oslo, Norway

sufficient for placement in moderately mechanically loaded bone [16], and the authors hypothesized that the TiO_2 scaffold may perform well in clinical use.

Sabetrasekh and co-workers [17] compared a TiO_2 scaffold to commercially available bone graft materials of natural and synthetic origin CaP, and titanium, and demonstrated different effects on cell viability and proliferation. However, the morphology of the tested graft materials in this study varied considerably and may be responsible for the variation in biological response. Few studies have compared similar morphology with different surface chemistry.

Therefore, the aim of the study was to compare the effect of SiO_2 or CaP coatings with TiO_2 on primary human osteoblasts in scaffolds of similar pore morphology.

2 Materials and Methods

2.1 Scaffold Production

Ceramic TiO_2 scaffolds were fabricated by a replication process [16]. In brief, TiO_2 slurry was prepared by dispersing 65 g of TiO_2 powder (Kronos 1171, Kronos Titan GmbH, Leverkusen, Germany) in 25 ml sterilised H_2O and the pH of the dispersion was kept at 1.5 for the entire duration of the stirring with small additions of 1 M HCl. The slurry was stirred (Dispermat CA-40, VMA-Getzmann GmbH, Germany) for 2.5 h at 5,000 rpm. Cylindrical polyurethane foam templates, 17 mm in diameter and 3.75 mm in height (60 ppi, Bulbren S, Eurofoam GmbH, Wiesbaden, Germany), were coated with the prepared slurry. Prior to sintering in 1,500 °C for 40 h, the polymer template was carefully burnt out of the green body at a lower temperature. 90 scaffolds were produced in total and divided into three groups of 30 scaffolds each. The final dimensions of the scaffolds were approximately 13.5 mm in diameter and 3 mm in height due to the shrinkage during the sintering phase. After relevant recoating procedures, all scaffold samples were steam sterilised in 121 °C for 20 min.

2.1.1 TiO_2

Sintered scaffolds were recoated with TiO_2 slurry prepared using the previously described procedure, only this time mixing 40 g of TiO_2 powder with 25 ml of water. Excess slurry was removed from the scaffold structure by centrifugation (1 min at 1,500 rpm; Biofuge 22R Heraeus Sepatech, Osterode, Germany). The recoated scaffolds were then sintered in 1,500 °C for 40 h.

2.1.2 SiO_2

SiO_2 slurry was prepared by dispersing 12 g of microcrystalline SiO_2 powder (Sigma-Aldrich, Steinheim, Germany) in 25 ml sterilised H_2O and stirred (Dispermat CA-40) for 2.5 h at 2,500 rpm. TiO_2 scaffolds were coated with SiO_2 by immersing the scaffolds in the prepared slurry. Excess slurry was centrifuged (1 min at 1,500 rpm; Biofuge 22R Heraeus Sepatech) out of the TiO_2 foam templates to ensure that only a thin layer of slurry covered the scaffold struts without blocking the pores. The SiO_2 coating layer was dried in 60 °C for 5 h and then heat treated at 1,200 °C for 5 h (LHT 02/17 LBR, Nabertherm GmbH, Lilienthal, Germany), the heating and cooling rates were set at 2.5 °C/min. The coating and heat treatment procedures were repeated once to apply two coating layers.

2.1.3 CaP

Calcium phosphate (CaP) coating was produced using sol–gel method [18]. 3 M triethyl phosphite ($C_2H_5O_3PO$; Sigma-Aldrich, Pittsburgh, PA, USA) dissolved in anhydrous ethanol was hydrolysed for 24 h with fixed amount of deionised water (the molar ratio between water and phosphite was fixed at 4:1) in a parafilm-sealed glass container under vigorous stirring. A stoichiometric amount of 3 M calcium nitrate ($Ca(NO_3)_2 \times 4H_2O$; Sigma-Aldrich) dissolved in anhydrous ethanol was added dropwise to the hydrolysed phosphite colloidal solution (sol) (Ca-to-P ratio fixed at 1.67:1). The mixed sol solution was then continuously agitated for additional 10 min and subsequently aged for 24 h at room temperature. TiO_2 scaffolds were dip coated with the prepared CaP sol, and excess sol was removed from the scaffolds by blowing pressurised air through the coated scaffolds to ensure that only a thin layer of sol covered the scaffold struts without blocking the pores. The CaP coating layer was dried in 80 °C for 10 h and then heat treated at 1,000 °C for 1 h (LHT 02/17 LBR), the heating and cooling rates were set at 2 °C/min. The dip coating and heat treatment procedures were repeated twice to apply three coating layers. For the purpose of XRD analysis, TiO_2 ceramic discs were dip coated in prepared CaP sol. The TiO_2 discs were prepared using the same slurry and heating cycle used in the production of the TiO_2 scaffolds.

2.2 Scaffold Characterisation

2.2.1 Pore Architecture

The initial visualisation and optical observation of the pore structure of the prepared scaffolds were performed using a scanning electron microscope (SEM) (TM-1000, Hitachi High-Technologies, Tokyo, Japan), and a desktop 1172 micro-computed tomography imaging system (micro-CT) (Skyscan, Kontich, Belgium) was used to determine the three-dimensional microstructure and porosity of the

scaffolds. All scans were performed with a voxel resolution of 8 μm. Otherwise all scanning and reconstruction (Nrecon, Skyscan) settings were performed as previously reported [16]. In order to eliminate potential edge effects, a cylindrical volume of interest (VOI) with a diameter of 8 mm and a height of 1.5 mm was selected in the centre of the scaffold. Pore architectural parameters were determined using the 3D analysis function in the standard Skyscan software (CTan, SkyScan).

2.2.2 *Chemical Surface Composition of Scaffolds*

The chemical compositions of the scaffold surfaces were investigated with energy-dispersive X-ray spectroscopy (EDX) using Quanta 200 FEG SEM (FEI, Denver, USA) equipped with EDX detector (EDAX, USA). The samples were scanned at environmental SEM mode with 15 kV acceleration voltage and 50 s acquisition time. The EDAX detector had a resolution of 132 eV.

X-ray diffraction (XRD) was used for additional chemical analysis of the CaP coating. XRD analysis was performed with D8 Discover powder diffractometer with a Ge (111) monochromator providing CuKα1 radiation and LynxEye detector (Bruker, Karlsruhe, Germany). The acquisition was done using $\theta - 2\theta$ configurations.

2.2.3 *Compressive Strength*

The mechanical strength was investigated in a compressive test (Zwicki, ZwickRoell, Ulm, Germany). The compression tests were performed in accordance with DIN EN ISO 3386 at room temperature using a load cell of 1 kN with preloading force set to be 0.5 N. The scaffolds were compressed along their long axes at a compression speed of 100 mm/min until failure. The force and displacement were recorded throughout the compression and converted to stress and strain based on the initial scaffold dimensions.

2.3 Cell Culture

The utilized cells were commercially available normal human osteoblasts (NHO) of two different donors (Cambrex Bio Science, Walkersville, MD, USA) from tibia and femur, respectively. The cells were grown in osteoblast growth media (OGM; Cambrex Bio Science), and the media was changed three times per week until confluence.

At the time of scaffold seeding, the NHO from tibia had reached passage 5 and the NHO from femur had reached passage 6. The scaffolds were placed in 24-well plates (Multidish, Nuncleon Surface, Nunc., Roskilde, Denmark). Triplicate of empty plastic wells served as untreated controls and triplicates of each scaffold were harvested at each time point.

The cells were seeded from a uniform solution in a dropwise manner (0.5 ml containing 18–25 $\times$ 10^3 cells) onto each scaffold. Further 0.5 ml of cell medium only was added to the wells after cell adhesion to ensure that all scaffolds were fully soaked. From this time the media was changed twice a week throughout the experiment.

At day 1, 7, 14, 21, 28, 35 and 42 cell culture media was sampled, and stored at −20 °C until analysis. At day 1, 14, 21, 28 and 42 the wells were washed in PBS prior to fixation in phosphate buffered formalin with a pH of 7.4.

2.4 Histological Analysis

The wells were immersed in an ascending alcohol solution prior to plastic embedding with a light-curing methacrylate resin (Technovit 7200 VLC, Heraeus Kulzer GmbH, Wehrheim, Germany). Slices containing parts of the cylindrical scaffolds were cut in either a vertical or horizontal direction using an Exakt saw (Exakt, Norderstedt, Germany). For the empty plastic wells, care was taken to include the well floor in the section. The histological sections were prepared according to the cutting-grinding technique previously described [19, 20]. The sections were grinded and polished (Polycut-S, Reichert-Jung, Leica Microsystems, Wetzlar, Switzerland) down to a thickness of approximately 50 μm and stained with hematoxylin and eosin, alizarin red or van Gieson. The histological sections were analysed to assess distribution of osteoblasts and mineralized nodules.

2.5 Cytokine and Chemokine Levels in Culture Medium: Immunoassay

Multianalyte profiling was performed using the Luminex 200^{TM} system and the XY Platform (Luminex, Corporation, Austin, TX, USA). Classification calibration microspheres were purchased from Luminex Corporation. Acquired fluorescence data were analysed by the 3.1 xPONENT software (Luminex). Prior to analysis, the samples were concentrated 5 times using Microsep Centrifugal tubes with 3 kDa cut-off (Pall Life Science, Ann Armor, MI, USA).

The concentrations of cytokines were determined using the 25-Milliplex Human Cytokine Immunoassay kit (Millipore, Billerica, MA, USA). Further, the level of bone markers interleukin-1β (IL-1β), interleukin-6 (IL-6), osteoprotegerin (OPG), osteocalcin (OC), leptin, osteopontin (OPN), parathyroid hormone (PTH), tumor necrosis factor-α (TNF-α), adrenocorticotropic hormone (ACTH), adiponectin and insulin were determined using Milliplex Human Bone Panel 1B Immunoassay kit (Millipore). All analyses were performed according to the manufacturers' protocols.

2.6 Total Protein Content

The total protein content (TP) was quantified with a BCA™ Protein Assay Kit (Pierce Biotechnology, Rockford, IL, USA) according to the manufacturer's instructions. The original cell media sample was diluted 1:5 prior to the analysis to fit the standard curve. This was determined using a spectrophotometer (NanoDrop, ND-1000, NanoDrop Products, Wilmington, DE, USA). 200 μL of the kit working reagent was added to 25 μL of each diluted sample. The absorbance was measured at 562 nm in a plate reader (Expert 96, Asys. Hitech GmbH, Eugendorf, Austria).

2.7 Alkaline Phosphatase Activity

Alkaline phosphatase (ALP) activity was quantified by measuring the cleavage of *p*-nitrophenyl phosphate (pNPP) (Sigma-Aldrich, St. Louis, MO, USA) into a soluble yellow end-product that absorbs at 405 nm. A standard curve was constructed with calf intestinal alkaline phosphatase (Promega, Madison, WI, USA). 25 μL of media was taken from each sample and incubated with 100 μL pNPP solution in a 96-well plate for 30 min in the dark at room temperature. 25 μL of 2 N NaOH was then added to each well to stop the reaction. The absorbance was measured in a plate reader (Expert 96).

2.8 Calcium Atomic Absorption Spectrophotometry

The Ca^{2+} concentration in the cell medium was assessed using a PerkinElmer 2380 flame atomic absorption spectrophotometer (PerkinElmer, Norwalk, CT, USA). 0.5 ml of a 3.6 % HCl solution was added to the cell medium and left for incubation with agitation on a plate shaker for 24 h. The next day a solution of 5 % lanthanum ($LaCl_3$) and 1 % HCl was added. The spectrophotometer was calibrated using a calcium concentration standard curve ranging from 0 to 5 ppm Ca^{2+}, created by the serial dilution of an atomic absorption calcium standard (Sigma Diagnostics, St. Louis, MO, USA).

2.9 Statistics

The data obtained by protein analyses and calcium atomic absorption spectrophotometry was compared between and within groups using Tukey's test following a parametric one way ANOVA. Where the equal variance and/or the normality test failed, a Kruskal–Wallis one way ANOVA on ranks was performed (SigmaPlot 12, Systat Software Inc, San Jose, USA). Mean and standard deviation are presented. A probability of <0.05 was considered significant.

3 Results

3.1 Scaffold Characterisation

All fabricated scaffolds showed an open and highly interconnected pore structure formed by spherical macropores, the average size of which exceeded 400 μm (Fig. 1). The average porosity of the scaffolds was 92 ± 2 % ($n = 6$)

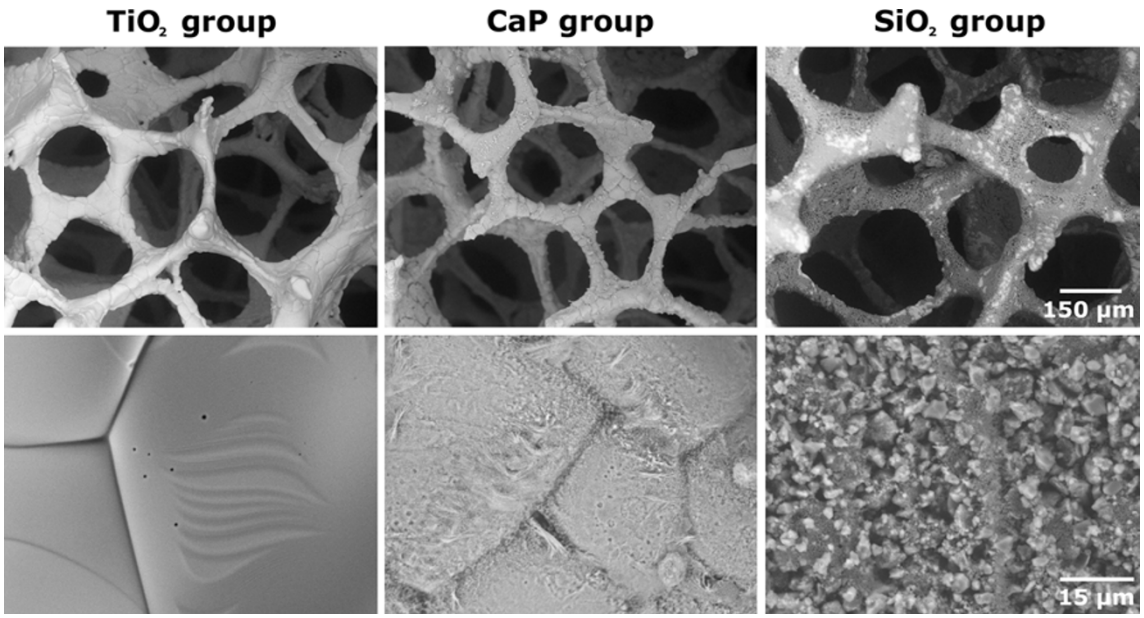

Fig. 1 Comparison of pore structure and surface morphology of the different scaffold groups

Table 1 Volumetric parameters (mean ± standard deviation) of the microCT morphological analysis for scaffolds coated with TiO_2 ($n = 6$)

Parameter	Unit	Mean	SD
Porosity	%	91.66	1.82
Surface area-to-volume ratio	l/mm	54.57	6.84
Pore size	μm	440.36	12.84
Strut thickness	μm	64.73	5.93
Intersection surface	mm^2	9.54	2.24
Interconnectivity <160 μm	%	95.81	1.09

and pore network showed over 95 % interconnectivity through connections as large as 160 μm. The volumetric scaffold parameters are listed in Table 1.

The thickness of the coating layer was estimated from SEM images to be approximately 1–3 μm for both CaP and SiO_2 coatings, and thus was not considered to affect the overall porosity or the pore architectural parameters, such as pore size, surface area-to-volume ratio, and interconnectivity. However, some closed pore walls were seen close to the bottom edge on some of the SiO_2 scaffolds. Due to limited thickness of the coating layer and the more radiolucent nature of CaP and SiO_2 coatings in comparison to TiO_2 bulk material, the coating layers were scarcely visible in micro-CT images.

While the pore structure of the scaffolds from the three different groups was regarded similar to each other, the scaffolds differed greatly in their surface properties. Typical surface morphologies of each of the three scaffold groups are presented in Fig. 1. The EDX analysis of the scaffold surfaces revealed that the surface of the TiO_2 scaffolds consisted of titanium and oxygen (Ti: 52 weight percentage (wt%), O: 46 wt%) with a small amount of aluminum impurities (2 wt%), while only silicon and oxygen was detected on the surface of SiO_2 coated scaffolds (Si: 48 wt%, O: 52 wt%). XRD pattern of the CaP coating revealed the chemical composition of the coating to match with calcium hydrogen phosphate hydroxide ($Ca_9HPO_4(PO_4)_5OH$) as shown in Fig. 2.

The TiO_2 coated scaffolds had the highest compressive strength. The compressive strength test results are listed in Table 2.

3.2 Histology

Several hundred sections were made in total, representing all harvest time points, all groups and both donors. Disappointingly, no mineralized nodules could be observed, and osteoblasts were scarce and only occasionally visible. The histological analysis was thus excluded from the study.

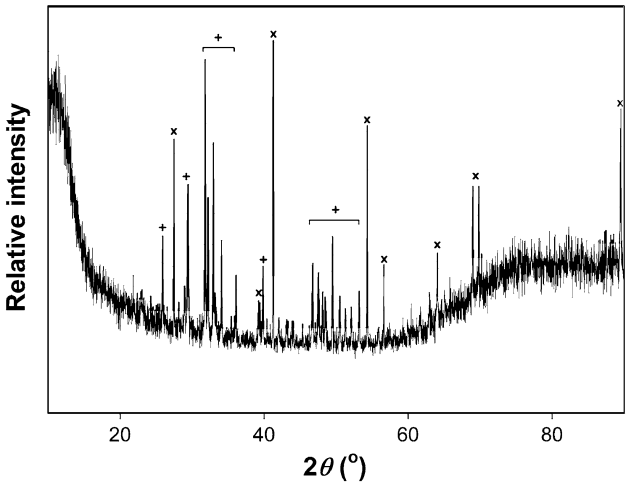

Fig. 2 XRD pattern of the CaP coating. Chemical composition of the coating identified the CaP as calcium hydrogen phosphate hydroxide. Rutile (TiO_2) (*times*) and $Ca_9HPO_4(PO_4)_5OH$ (*plus*)

Table 2 Compressive strength (mean ± standard deviation) ($n = 5$)

Coating	Unit	Mean	SD
TiO_2	MPa	1.43	0.11
SiO_2	MPa	0.34	0.06
CaP	MPa	0.25	0.03

3.3 Enhanced Secretion of OPN and OPG from Cells on TiO_2

The level of IL-1β, PTH, TNF-α, ACTH, adiponectin and insulin were all below reliable detection and the level of leptin was detected in the femur donor only.

The secretion of leptin was similar for all treatment groups until day 42 where the secretion from cells on TiO_2 were higher than on CaP and SiO_2 ($P = 0.016$, $P = 0.015$, respectively). No difference was observed at any time point between TiO_2 and plastic (data not shown).

There were no differences in the secretion of OC from cell cultures in the different scaffolds (data not shown).

The secretion of OPN from both tibia and femur osteoblasts were higher on TiO_2 than from those on CaP and SiO_2 at day 7 ($P = 0.013$, $P = 0.043$ and $P < 0.001$, $P = 0.001$, respectively), day 14 ($P < 0.001$, $P = 0.002$ and $P = 0.003$, $P = 0.014$, respectively), day 21 ($P = 0.003$, $P = 0.008$ and $P < 0.001$, $P = 0.012$, respectively), and in the femur donor only at day 28 ($P < 0.001$, $P = 0.001$, respectively) and at day 42 (both $P < 0.001$) (Fig. 3).

Cells on CaP had no change in the secretion of OPN, and was significantly lower than the secretion from cells on SiO_2 in femur at day 28 ($P = 0.046$).

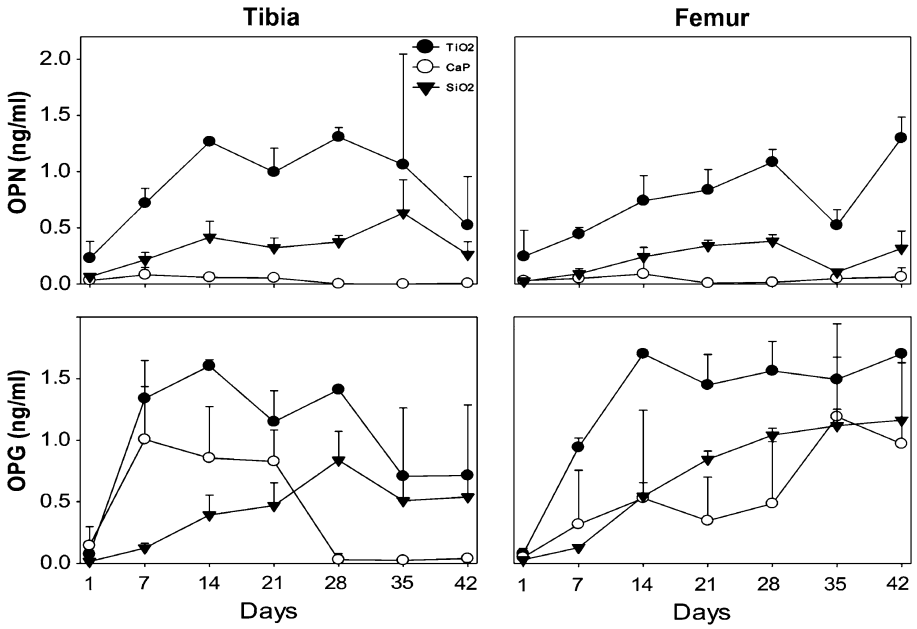

Fig. 3 The mean concentration (ng/ml) of OPN and OPG in cell culture media from primary human osteoblasts from tibia (*left column*) and femur (*right column*) at each time point (days). The *error bars* represent the standard deviation of the mean ($n = 3$).
CaP = $Ca_9HPO_4(PO_4)_5OH$

The secretion of OPN from osteoblasts, both from tibia and femur, was enhanced on plastic during the study period (day 1; 0.32 ± 0.09 ng/ml and 0.31 ± 0.06 ng/ml, respectively, day 7; 1.54 ± 0.34 ng/ml and 1.1 ± 0.07 ng/ml, respectively, and day 14; 2.38 ± 0.25 ng/ml and 1.2 ± 0.08 ng/ml, respectively). The secretion of OPN from cells on TiO_2, however, was lower than the secretion from control cells at day 7 ($P = 0.003$ and $P < 0.001$, for tibia and femur osteoblasts, respectively), day 14 ($P < 0.001$ and $P = 0.02$, respectively), and day 28 ($P = 0.034$) in the femur donor only. After day 28 there is no significant difference between the secretions from cells on plastic compared to TiO_2.

The concentration of OPG was enhanced in all groups (Fig. 3). The secretion of OPG from tibia osteoblasts on TiO_2 was higher than from cells on SiO_2 at day 7 ($P = 0.017$) and day 14 ($P = 0.008$), and the secretion from femur osteoblasts on TiO_2 was higher than from cells on CaP and SiO_2 at day 14 ($P = 0.023$ and $P = 0.025$, respectively), day 21 ($P = 0.001$ and $P = 0.039$, respectively), and at day 28 compared to CaP only ($P = 0.007$). On plastic, the OPG secretion from tibia and femur osteoblasts were 0.22 ± 0.001 and 0.32 ± 0.01 ng/ml, respectively, at day 1, and 1.78 ± 0.36 and 1.11 ± 0.04 ng/ml, respectively, at day 7. The secretion of OPG on plastic, however, was significantly higher than TiO_2 only in the femur donor at day 1 ($P < 0.001$).

3.4 Enhanced Secretion of IL-6 and Rantes from Cells on TiO_2

The secretion of IL-6 from tibia osteoblasts on TiO_2 was higher than from cells on CaP ($P < 0.001$) and SiO_2 ($P < 0.001$) at day 28 only. The secretion of IL-6 from femur osteoblasts was higher compared to from cells on CaP at day 21 ($P = 0.003$) (Fig. 4).

The secretion of IL-6 was enhanced from both tibia and femur osteoblasts on plastic (day 1; 224 ± 18 and 274 ± 34 pg/ml, respectively, day 7; 378 ± 61 and 403 ± 83 pg/ml, respectively, and day 14; 545 ± 135 and 560 ± 0 pg/ml, respectively). The IL-6 secretion from cells on plastic was higher than the secretion on TiO_2 in cells of tibia origin only at day 21 ($P = 0.003$) and day 28 ($P < 0.001$).

There were no differences in the secretion of IL-4 from cells on TiO_2 and CaP. In comparison the secretion from tibia and femur osteoblasts on SiO_2 were notably lower than on both TiO_2 and CaP the first 14 days (day 1; $P = 0.002$, $P = 0.002$ and $P = 0.009$, $P = 0.023$, respectively, day 7; $P < 0.001$ for all, and day 14, $P < 0.001$, $P < 0.001$ and $P = 0.024$, $P = 0.006$, respectively) (Fig. 4). There were no significant difference in the secretion from cells on TiO_2 and plastic. A similar pattern of secretion was observed for IL-8, with no differences between cells cultured on plastic, TiO_2 or CaP, but a reduced secreted level from cells on SiO_2 the first time points (data not shown).

The secretion of RANTES was enhanced from both tibia and femur osteoblasts on TiO2 from day 1; 0.6 ± 0.04 and 1.4 ± 0.6 pg/ml, respectively, to day 42; 3.1 ± 0.6 and 10.5 ± 4 pg/ml, respectively (Fig. 4). The secretion of RANTES from tibia osteoblasts was higher on TiO_2 than from cells on SiO_2 at day 7 ($P = 0.004$), and both CaP and SiO_2 at day 14 ($P = 0.002$, $P = 0.022$, respectively). Femur osteoblasts secreted higher levels on TiO_2 compared to CaP and SiO_2 at day 21 only ($P = 0.006$, $P = 0.021$,

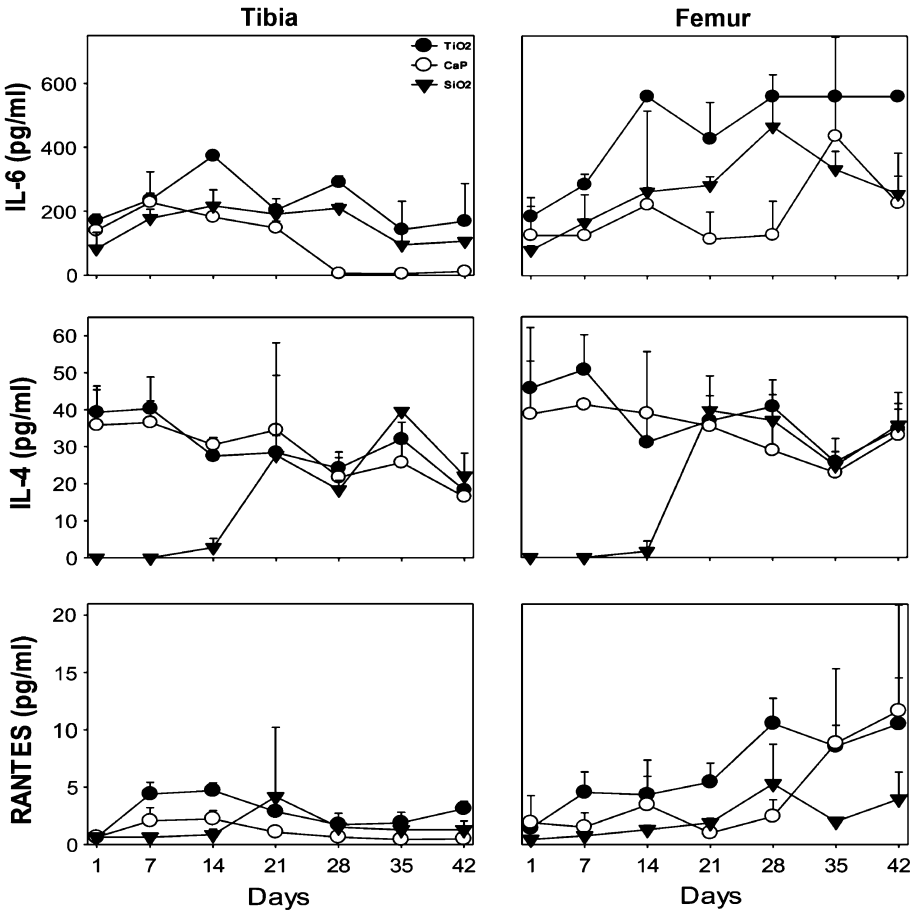

Fig. 4 The mean concentration (pg/ml) of IL-6, IL-4 and RANTES in cell culture media from primary human osteoblasts from tibia (*left column*) and femur (*right column*) at each time point (days). The *error bars* represent the standard deviation of the mean ($n = 3$). CaP = $Ca_9HPO_4(PO_4)_5OH$

respectively). No difference was observed at any time point in either donor comparing TiO_2 and plastic.

3.5 Angiogenic Markers

The secreted levels of MCP-1 were higher from cells on TiO_2 and SiO_2 compared to from cells on CaP (Fig. 5). However, the difference was not significant for other time points than day 28 in the tibia donor (TiO_2: $P < 0.001$ and SiO_2: $P < 0.001$).

The secretion of MCP-1 was enhanced for cells in both the tibia and femur donor on plastic (from day 1; 0.25 ± 0.01 and 0.7 ± 0.02 ng/ml, respectively, to day 7; 0.9 ± 0.01 and 1.1 ± 0.02 ng/ml, respectively). The MCP-1 secretion from cells on plastic was similar to that of cells on TiO_2, and a difference was observed at day 1 in the femur donor only ($P = 0.008$).

The secretion of VEGF was enhanced from femur osteoblasts on TiO_2 from day 1; 0.03 ± 0.01, to day 42; 0.6 ± 0.08 ng/ml (Fig. 5), and secretion was higher than from cells on SiO_2 at day 7 ($P = 0.045$), CaP at day 14 ($P = 0.028$), CaP and SiO_2 at day 21 ($P < 0.001$, $P < 0.001$, respectively), day 28 ($P < 0.001$, $P = 0.004$, respectively) and day 42 ($P < 0.001$, $P < 0.001$, respectively). No significant differences were observed in the tibia donor and no difference was observed at any time point for either donor between TiO_2 and plastic.

3.6 Alkaline Phosphatase

The ALP activity of day 1 was similar to that of day 42 for all groups in both donors, and ALP was secreted in a steady-state throughout the 6 weeks on all scaffolds and plastic (data not shown).

3.7 Total Protein Content

There was no difference in TP secretion among groups in either donor. Osteoblasts from tibia demonstrated a threefold increase of the TP concentration from day 1 to the end of the experiment, whereas osteoblasts from femur displayed a minor increase only. Plastic did not exhibit any difference compared to the test groups at any time in either donor (data not shown).

3.8 Ca^{2+}

The secretion of Ca^{2+} was not altered in cells from either the tibia or femur donor on plastic, TiO_2 or SiO_2 (data not

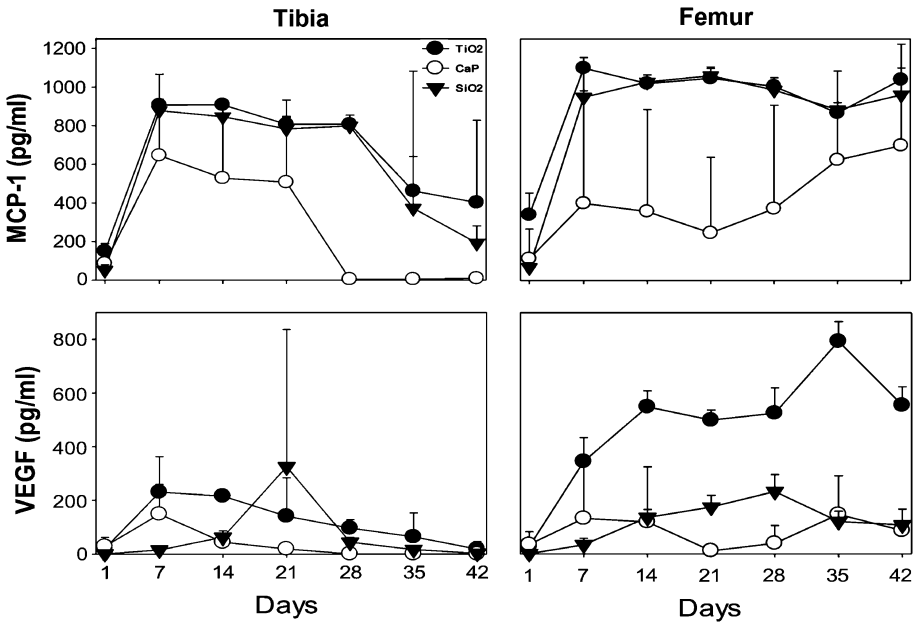

Fig. 5 The mean concentration (pg/ml) of MCP-1 and VEGF in cell culture media from primary human osteoblasts from tibia (*left column*) and femur (*right column*) at each time point (days). The *error bars* represent the standard deviation of the mean ($n = 3$).
CaP = $Ca_9HPO_4(PO_4)_5OH$

shown). An initial high concentration was, however, found in the cell culture media from tibia osteoblasts on CaP at day 1 and 7 ($P < 0.001$) compared to all other groups, and in osteoblasts from femur compared to TiO_2, SiO_2 and plastic at day 1 ($P = 0.004$, $P = 0.005$, $P = 0.004$, respectively) and at day 7 ($P < 0.001$, $P = 0.003$, $P = 0.002$, respectively).

4 Discussion

The TiO_2 coating induced a higher osteoblast secretion of OPN, OPG, IL-6, RANTES and VEGF compared to CaP and SiO_2 coatings. The two latter coatings did not induce significantly higher secretion of any detectable cytokine at any single time point compared to the TiO_2 coated group. Thus, TiO_2 coated scaffolds demonstrated osteoblast secretion levels closer to the control, although neither tested coating could display osteoblast secretion higher than that of the control for any cytokine at any single time point.

Webster and co-workers [21] compared rat osteoblast function on discs of TiO_2, alumina, hydroxyapatite and borosilicate. Although the study aimed to evaluate ceramic grain size, nanophase TiO_2 induced higher levels of ALP and Ca^{2+} compared to hydroxyapatite and borosilicate. The cell density was similar on TiO_2 and hydroxyapatite at 5 days, both higher than borosilicate, whereas the cells were more spread on borosilicate compared to TiO_2 and hydroxyapatite.

The results suggested that nanophase TiO_2 support rat osteoblast differentiation better than borosilicate and hydroxyapatite. Similarly, TiO_2 supported higher secretion of osteoblastic markers compared to calcium phosphate and silica in the present study. Although no differences were observed in ALP activity and the Ca^{2+} release only differed the first week, the level of other markers suggested enhanced osteoblast differentiation. Regarding cell proliferation, Webster and co-workers [21] found higher cell density in the TiO_2 and hydroxyapatite groups compared to the borosilicate control at day 3 and 5. In the present study no difference in total protein content was observed. However, these methods of evaluating cell proliferation vary considerably, and may not be comparable. Detection of significant differences in the total protein content in cell media consisting of foetal calf serum require great variation, especially if the cell number is low.

Sabetrasekh et al. [17] evaluated cell proliferation using human mesenchymal stem cells cultured on TiO_2 granules and compared it to other bone graft substitute granules, one consisting of hydroxyapatite and one of hydroxyapatite and β-tricalcium phosphate in a 60:40 ratio. The cell number was significantly higher on TiO_2 compared to the calcium phosphates at both day 1 and day 3. Again the cell proliferation methodology may not be compared to the present study. The results of these studies suggest that other analyses should be employed in further research to detect significant differences in cell proliferation.

Although the porosity and interconnectivity was similar across the differently coated scaffolds, the surface roughness was different for the three coatings (Fig. 1). It has been demonstrated that cell differentiation is sensitive to both micro- and submicroscale surface roughness, and increased roughness is associated with enhanced osteoblast differentiation and local factor production in vitro [22, 23]. Thus, other than the chemistry of the coating material, the

difference in surface roughness may therefore have attributed to the results. However, the TiO_2 coated scaffolds had the smoothest surface, yet higher secretion, suggesting that the chemistry of the coating materials indeed had significant impact.

The XRD analysis demonstrated the CaP material to be $Ca_9HPO_4(PO_4)_5OH$, known as calcium-deficient hydroxyapatite. This material has been described previously, and has been reported to have properties comparable to β-tricalcium phosphate with regard to osteogenic induction [24]. CaP demonstrated higher concentrations of Ca^{2+} ions at the first two time points in both donors. This was probably due to passive dissolution of Ca^{2+} ions from the CaP material the first week, which has been reported previously [25, 26]. As the cells on CaP coated scaffolds reached the steady-state concentration of Ca^{2+} ions observed in the other groups by day 14, this may suggest that by then the dissolution had reached equilibrium. The dissolution of calcium did not, however, seem to enhance expression of osteoblastic markers as previously suggested [27, 28].

The histological analysis did not contribute to any results. However, the absence of mineralized nodules was in agreement with the non-detectable changes in the concentrations of OC, Ca^{2+} and ALP activity, indicating that mineralization did not take place. Alizarin red and van Gieson staining were also performed as the hematoxylin and eosin stain did not render measurable results, but with the same outcome. The histological analysis suggests there may have been too few cells in the experiment. A three-dimensional scaffold may necessitate a higher quantity of cells in order to observe proper mineralization. The lack of mineralized nodules observed on plastic may further suggest a low cell number. The chosen methodology of plastic embedding and grinding prior to histological analysis may not have been appropriate for the in vitro experiment performed.

Zhou and co-workers [29] found that a small seeding density of human alveolar osteoblasts on mPCL-TCP scaffolds could support cell attachment and proliferation, secretion of OC and ALP, as well as extracellular matrix synthesis. Further, the authors observed that seeding at higher densities did not influence the extent of cell proliferation and tissue formation over time. However, the lowest cell density tested in that study was 5×10^4 million cells per scaffold, utilizing a scaffold size of $3 \times 3 \times 5$ mm^2. The cell density in the present study was in comparison 1.8–2.5 $\times$ 10^4 million, cultured on considerably larger scaffolds of 13.5 mm in diameter and 3 mm in height. This may suggest that the cell density was too small for a large three-dimensional substrate in order to achieve significant variation in OC and ALP levels, and histologically detectable mineralization. On the other hand, osteoblasts cultured on plastic did render similar results as the test groups, despite the lower total surface area. As mineralization was not evident in any scaffold or on plastic, it is tempting to suggest that the results would have been different with a higher cell seeding number. In the present study a static culture condition was employed. A dynamic culture condition in combination with a higher cell seeding number may further modify the outcome. This has previously been reported to improve cell invasion and cellular attachment inside plastic and titanium scaffolds [30, 31], but will have to be confirmed by further in vitro experiments.

5 Conclusions

A higher secretion of bone markers (OPN, OPG), immune modulators (IL-6, RANTES) and angiogenic markers (VEGF) indicate that TiO_2 support osteoblast growth and bone remodeling better than CaP and SiO_2. This study demonstrates that TiO_2 scaffolds are able to induce human osteoblast differentiation in vitro, suggesting its potential as a scaffold for hard tissue repair.

Acknowledgments This study was supported by Eureka-Eurostars Project Application E!5069 NewBone. We appreciate the excellent technical assistance from Aina Mari Lian, Grazyna Jonski and Britt Mari Kvam (Faculty of Dentistry, Oral Research Laboratory, University of Oslo, Norway).

References

1. Zimmermann G, Moghaddam A (2011) Int J Care Injured 42:S16–S21
2. Younger EM, Chapman MW (1989) J Orthop Trauma 3(3):192–195
3. Jones JR, Ehrenfried LM, Hench LL (2006) Biomaterials 27(7):964–973
4. Torres F, Nazhat S, Sheikh Md Fadzullah SH, Maquet V, Boccaccini A (2007) Compos Sci Technol 67(6):1139–1147
5. Lu JX, Flautre B, Anselme K, Hardouin P, Gallur A, Descamps M, Thierry B (1999) J Mater Sci Mater Med 10(2):111–120
6. Dorozhkin S (2010) Biomaterials 31(7):1465–1485
7. Ripamonti U (1996) Biomaterials 17(1):31–35
8. Yuan H, Kurashina K, de Bruijn JD, Li Y, de Groot K, Zhang X (1999) Biomaterials 20(19):1799–1806
9. Yuan H, de Bruijn JD, Zhang X, van Blitterswijk CA, de Groot K (2001) J Biomed Mater Res 58(3):270–276
10. Chen QZ, Thompson ID, Boccaccini AR (2006) Biomaterials 27(11):2414–2425
11. Benaqqa C, Chevalier J, Saadaoui M, Fantozzi G (2005) Biomaterials 26(31):6106–6112

12. Bretcanu O, Chen Q, Misra SK, Boccaccini AR, Roy I, Verne E, Brovarone CV (2007) Glass Technol Eur J Glass Sci Technol A 48(5):227–234
13. Suchanek W, Yoshimura M (2011) J Mater Res 13(1):94–117
14. Jokinen M, Pätsi M, Rahiala H, Peltola T, Ritala M, Rosenholm JB (1998) J Biomed Mater Res 42(2):295–302
15. Nygren H, Tengvall P, Lundström I (1997) J Biomed Mater Res 34(4):487–492
16. Tiainen H, Lyngstadaas SP, Ellingsen JE, Haugen HJ (2010) J Mater Sci Mater Med 21(10):2783–2792
17. Sabetrasekh R, Tiainen H, Lyngstadaas SP, Reseland J, Haugen H (2011) J Biomater Appl 25(6):559–580
18. Liu D-M, Yang Q, Troczynski T (2002) Biomaterials 23(3):691–698
19. Donath K, Breuner G (1982) J Oral Pathol 11(4):318–326
20. Rohrer MD, Schubert CC (1992) Oral Surg Oral Med Oral Pathol 74(1):73–78
21. Webster TJ, Ergun C, Doremus RH, Siegel RW, Bizios R (2000) Biomaterials 21(17):1803–1810
22. Kieswetter K, Schwartz Z, Hummert T, Cochran D, Simpson J, Dean D, Boyan B (1996) J Biomed Mat Res 32(1):55–63
23. Kubo K, Tsukimura N, Iwasa F, Ueno T, Saruwatari L, Aita H, Chiou W-A, Ogawa T (2009) Biomaterials 30(29):5319–5329
24. Kasten P, Luginbühl R, van Griensven M, Barkhausen T, Krettek C, Bohner M, Bosch U (2003) Biomaterials 24(15):2593–2603
25. Drevet R, Velard F, Potiron S, Laurent-Maquin D, Benhayoune H (2011) J Mater Sci Mater Med 22(4):753–761
26. Zhang Q, Chen J, Feng J, Cao Y, Deng C, Zhang X (2003) Biomaterials 24(26):4741–4748
27. Choudhary S, Wadhwa S, Raisz LG, Alander C, Pilbeam CC (2003) J Bone Miner Res 18(10):1813–1824
28. Chuenjitkuntaworn B, Inrung W, Damrongsri D, Mekaapiruk K, Supaphol P, Pavasant P (2010) J Biomed Mater Res Part A 94(1):241–251
29. Zhou YF, Sae-Lim V, Chou AM, Hutmacher DW, Lim TM (2006) J Biomed Mater Res Part A 78(1):183–193
30. Granet C, Laroche N, Vico L, Alexandre C, Lafage-Proust MH (1998) Med Biol Eng Comput 36(4):513–519
31. van den Dolder J, Spauwen PHM, Jansen JA (2003) Tissue Eng 9(2):315–325